UNIVERSITY OF AMSTERDAM

UvA-DARE (Digital Academic Repository)

Absorption coefficient of metal-containing photoresists in the extreme ultraviolet

Fallica, R.; Haitjema, J.; Wu, L.; Castellanos Ortega, S.; Brouwer, A.M.; Ekinci, Y.

DOI
10.1117/1.JMM.17.2.023505

Publication date
2018

Document Version
Final published version

Published in
Journal of Micro/Nanolithography, MEMS and MOEMS

License
Article 25fa Dutch Copyright Act (https://www.openaccess.nl/en/policies/open-access-in-dutch-copyright-law-taverne-amendment)

Link to publication

Citation for published version (APA):
Fallica, R., Haitjema, J., Wu, L., Castellanos Ortega, S., Brouwer, A. M., & Ekinci, Y. (2018). Absorption coefficient of metal-containing photoresists in the extreme ultraviolet. *Journal of Micro/Nanolithography, MEMS and MOEMS*, *17*(2), Article 023505. https://doi.org/10.1117/1.JMM.17.2.023505

General rights
It is not permitted to download or to forward/distribute the text or part of it without the consent of the author(s) and/or copyright holder(s), other than for strictly personal, individual use, unless the work is under an open content license (like Creative Commons).

Disclaimer/Complaints regulations
If you believe that digital publication of certain material infringes any of your rights or (privacy) interests, please let the Library know, stating your reasons. In case of a legitimate complaint, the Library will make the material inaccessible and/or remove it from the website. Please Ask the Library: https://uba.uva.nl/en/contact, or a letter to: Library of the University of Amsterdam, Secretariat, P.O. Box 19185, 1000 GD Amsterdam, The Netherlands. You will be contacted as soon as possible.

UvA-DARE is a service provided by the library of the University of Amsterdam (https://dare.uva.nl)

Download date:10 Sept 2026

Journal of
Micro/Nanolithography,
MEMS, and MOEMS

Nanolithography.SPIEDigitalLibrary.org

Absorption coefficient of metal-containing photoresists in the extreme ultraviolet

Roberto Fallica
Jarich Haitjema
Lianjia Wu
Sonia Castellanos
Albert M. Brouwer
Yasin Ekinci

SPIE.

Roberto Fallica, Jarich Haitjema, Lianjia Wu, Sonia Castellanos, Albert M. Brouwer, Yasin Ekinci, "Absorption coefficient of metal-containing photoresists in the extreme ultraviolet," *J. Micro/Nanolith. MEMS MOEMS* **17**(2), 023505 (2018), doi: 10.1117/1.JMM.17.2.023505.

Downloaded From: https://www.spiedigitallibrary.org/journals/Journal-of-Micro/Nanolithography,-MEMS,-and-MOEMS on 08 May 2019
Terms of Use: https://www.spiedigitallibrary.org/terms-of-use

Absorption coefficient of metal-containing photoresists in the extreme ultraviolet

Roberto Fallica,[a,*] Jarich Haitjema,[b] Lianjia Wu,[b] Sonia Castellanos,[b] Albert M. Brouwer,[b,c] and Yasin Ekinci[a]
[a]Paul Scherrer Institute, Villigen, Switzerland
[b]Advanced Research Center for Nanolithography, Amsterdam, The Netherlands
[c]University of Amsterdam, van 't Hoff Institute for Molecular Sciences, Amsterdam, The Netherlands

Abstract. The amount of absorbed light in thin photoresist films is a key parameter in photolithographic processing, but its experimental measurement is not straightforward. The optical absorption of metal oxide-based thin photoresist films for extreme ultraviolet (EUV) lithography was measured using an established methodology based on synchrotron light. Three types of materials were investigated: tin cage molecules, zirconium oxoclusters, and hafnium oxoclusters. The tin-containing compound was demonstrated to have optical absorption up to three times higher than conventional organic-based photoresists have. The absorptivity of the zirconium oxocluster was comparable to that of organic polymer-based photoresists, owing to the low absorption cross section of zirconium at EUV. The hafnium-containing resist shows about twice as high absorptivity as an organic photoresist, owing to the significantly higher absorbance of hafnium. From the chemical composition and crystal structure, the density of the spin-coated films was determined. Using the density of the films and the tabulated data for atomic cross section at EUV, the expected absorptivity of these resists was calculated and discussed in comparison to the experimental results. The agreement between measured and expected absorption was fairly good with some substantial discrepancies due to differences in the actual film density or to thickness inhomogeneity due to the spin coating. The developed method here enables the accurate measurement of the EUV absorption of the photoresists and can contribute to the further development of EUV resists and more accurate lithographic modeling. © *2018 Society of Photo-Optical Instrumentation Engineers (SPIE)* [DOI: 10.1117/1.JMM.17.2.023505]

Keywords: extreme ultraviolet; absorption; ligand; tin cage; oxocluster; metal oxide; photoresist; stochastics.

Paper 18017P received Jan. 30, 2018; accepted for publication Apr. 12, 2018; published online May 10, 2018.

1 Introduction

In a lithographic process, the ideal amount of light absorbed in a photoresist film is a tradeoff between two competing requirements. On one hand, the photoresist should have high transmissivity in order to be exposed uniformly and avoid tapering effects throughout its depth. On the other hand, the efficient use of the incoming radiation requires films to absorb as much light as possible. Photoresists for visible and *i*-line photolithography are based mostly on diazonaphthoquinone (DNQ) and novolak resins compounds.[1] These materials were designed to coat at micrometric thickness, and, therefore, their absorptivity is relatively low and most of the light is transmitted through the film. Deep ultraviolet (DUV) photolithography operates at 248- and 193-nm wavelength and uses chemically amplified resists (CARs) based on an organic polymer backbone. CAR materials for 248-nm DUV technology had linear absorption coefficient between 0.2 and 1 μm^{-1} and typical coating thickness of 300 to 800 nm, which resulted in more than 80% of the incoming light being transmitted through the film.[2,3] In current 193-nm wavelength DUV lithography, photoresists absorb more (1 to 3 μm^{-1}) and typically coat at about 100 nm[3–5] to achieve high-resolution patterning: with these features, a reasonable tradeoff between transmitted and absorbed light is maintained.

As the photolithography technology transitions to the extreme ultraviolet (EUV) regime for next-generation high-volume manufacturing of semiconductor devices, new challenges arise for photoresist materials.[6] In particular, less than 1/10 the number of EUV photons is needed to deliver the same incident dose than using DUV photons, and reflection is negligible while absorption is prevailing. The photochemistry of resist exposure at EUV wavelength (13.5 nm) is radically different[7] to previous technologies. In addition, interaction between light at EUV wavelength and electronic states of elements can be remarkably stronger than the interaction of DUV light with molecular materials. As a result, EUV light can be strongly absorbed by matter. The pursuit of ever higher lithographic resolution requires the use of substantially thinner coatings (≈35 nm) in EUV than it used to be for DUV to prevent pattern collapse. Nevertheless, a 35-nm-thick organic photoresist film with typical absorption 4.8 μm^{-1} would still only exploit about 15% of the incident light. This consideration is critical for the economy of high-volume manufacturing because EUV light is costly to generate, and EUV sources based on tin plasma have low efficiency (≈5%) and limited collector lifetime.[8]

Moreover, further challenges remain.[6] For instance, the resolution-linewidth roughness-sensitivity tradeoff postulates that these three characteristics cannot be improved simultaneously owing to the mutual dependencies among one another,[9] which sets an insurmountable limitation to CAR. Entirely new approaches in photoresists' functionality

*Address all correspondence to: Roberto Fallica, E-mail: roberto.fallica@psi.ch

1932-5150/2018/$25.00 © 2018 SPIE

Downloaded From: https://www.spiedigitallibrary.org/journals/Journal-of-Micro/Nanolithography,-MEMS,-and-MOEMS on 08 May 2019
Terms of Use: https://www.spiedigitallibrary.org/terms-of-use

and synthesis are instead being undertaken, among which hybrid organometallic photoresists,[10] oxide nanoparticles,[11,12] and condensed molecular oxides,[6,13] testify to the intense scientific research in this field. In particular, hybrid oxide resists that are synthesized from metallic elements and/or high Z-number elements have shown a remarkable combination of features (high resolution, high etch resistance, and compatibility with existing processes) that makes them promising for EUV lithography.[6] A significant drawback of the metal oxide platform is the lack of chemical amplification. Because the condensation reaction is not catalyzed by photoacid generator, early prototypes of this class showed poor sensitivity and required EUV doses in excess of 50 mJ/cm^2 to be patterned,[14] which is well beyond the target dose (<20 mJ/cm^2) that is specified for the required high throughput in industrial EUV scanners.[15] Recent improvements in the synthesis are addressing this issue by tuning the organic ligand, the exposure chemistry, and the optical absorptivity.[6]

Absorption of EUV light in matter depends entirely on the atomic composition and the absorption cross section of elements (reported in Fig. 1 from tabulated data[16]) shows large differences. The most promising elements for incorporation in a photoresist to enhance optical absorption are those transition metals, and metals or semimetals with large atomic number whose deep semicore orbitals have large interaction cross section with EUV photons.

Enhanced optical absorption also brings the advantage of higher lithographic sensitivity, which could, in part, compensate the lack of chemical amplification although, in this regard, several other parameters play a role. For instance, the stochastic variations due to the relatively low number of EUV photons for a given exposure dose, and the microscopic fluctuations in the density of the components of the CAR (such as photoacid generator and quencher), are critical issues that narrow the process window. Since photon shot noise is proportional to the reciprocal of the square root of the amount of absorbed photons and because metal resists have higher absorptivity and fewer (or even single) components, the stochastics is reduced. For further improvement of the sensitivity—in addition to enhanced absorption—chemical amplification can also be integrated into metal resists. This is not straightforward in single molecular metal oxide photoresist, and very few such systems have been reported so far.[17] As a result, the lithographic sensitivity of metal oxides has been consistently reported to be below that of polymer-based CAR.

Very few experimental measurement experiments on the absorption coefficient of photoresist materials have been previously reported in the EUV range.[18–21] In one of those pioneering works, it was reported that the transmissivity of a photoresist at EUV is correlated to the amount of incorporated tellurium.[18] Several reasons make the direct measurement of absorption in thin films challenging. Since the EUV is strongly absorbed by matter, a sufficiently bright and stable source is needed to get a measurable signal in transmission mode, which is more difficult, at EUV, than it is at longer wavelengths. Moreover, the absorption of the photoresist should be measured in coated form, similarly to the actual exposure conditions. The substrate of the thin film should be transparent to EUV, which means a free-standing membrane of thickness less than a micron has to be used. Finally, the extraction of the absorption coefficient α requires the accurate measurement of the thickness of the spin-coated film.

We have recently developed a methodology to measure the absorption of thin photoresist films using EUV light from a synchrotron source in transmission mode.[22] Our experimental setup allows the extraction of the absorption coefficient from the measurement of the transmissivity of thin photoresist films and their thickness while accounting for all sources of uncertainty in the measurement. In this work, we investigate the absorption coefficient of nonproprietary metal-based photoresists. These materials are based on tin cage structures and on zirconium and hafnium oxoclusters, which have been described in detail.[23] The materials data (composition and density) are therefore used to accurately calculate the expected absorption and to carry out a comparison to the experimental results.

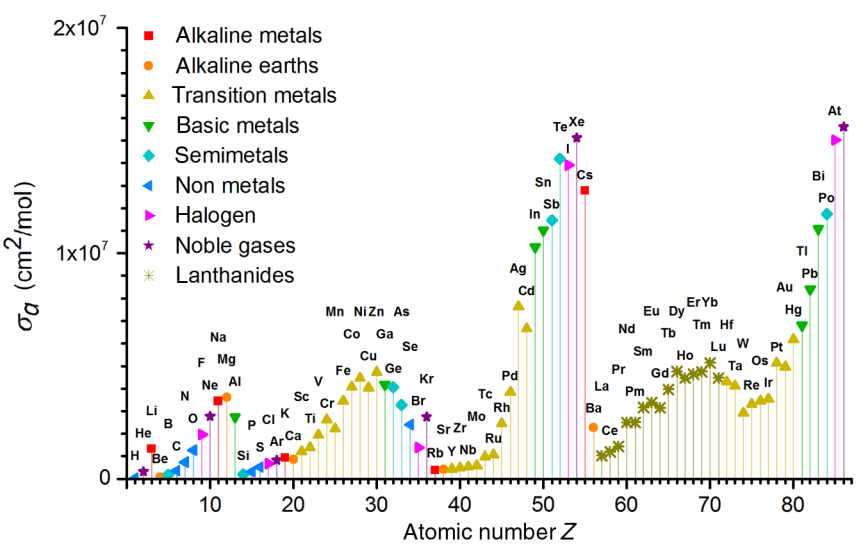

Fig. 1 Atomic absorption cross section σ_a at EUV ($\lambda = 13.5$ nm) of elements with atomic number Z from 1 to 86, plotted from tabulated data.[16]

Downloaded From: https://www.spiedigitallibrary.org/journals/Journal-of-Micro/Nanolithography,-MEMS,-and-MOEMS on 08 May 2019
Terms of Use: https://www.spiedigitallibrary.org/terms-of-use

Fig. 2 Schematic of experimental setup for absorption measurement at the XIL beamline.

2 Experimental Details

2.1 *EUV Transmittance Measurement at the XIL-II Beamline*

The XIL-II beamline of the Swiss Light Source operates at EUV light of 13.5-nm wavelength from a synchrotron source. The average flux is in excess of 30 mW/cm^2. The beamline is mainly used for EUV interference lithography[24] and actinic mask inspection.[25] The beam is generated by the undulator source and focused to a spatial filter pinhole of 30-μm diameter and expands about 12 m, resulting in a relatively homogeneous beam over several millimeters. A square open-frame mask (0.5×0.5 mm^2) is located in front of the sample. The transmittance measurement is carried out in an experimental setup developed in our previous work and shown schematically in Fig. 2.[22] An AXUV100G silicon photodiode is located behind the sample, and its photocurrent is collected using a Keithley 6430 amperometer. Because the membrane itself absorbs EUV light, the net flux I_0 is calibrated by measuring the transmittance of a blank SiN_x membrane. Finally, the transmittance T_X of the thin photoresist film is given by the ratio between measured photocurrent I and the reference photocurrent I_0.

2.2 *Linear Absorption Coefficient*

As the Beer–Lambert law describes, the amount of light transmitted through a homogeneous medium is a function of the thickness of the medium d and of the linear absorption coefficient α

$$T_X = e^{-\alpha d}. \tag{1}$$

From Eq. (1), the linear absorption coefficient of the pristine, unexposed material can be calculated in our experimental setup in transmission mode as

$$\alpha = -\frac{1}{d} \ln \frac{I(t_0)}{I_0} (\mu\text{m}^{-1}), \tag{2}$$

where I_0 is the photocurrent through a blank membrane and $I(t_0)$ is the photocurrent through the photoresist/membrane stack at the beginning of the exposure ($t = t_0$).

2.3 *Samples Preparation and Description*

Silicon nitride (SiN_x) membranes (100 nm nominal thickness, 3×3 mm^2) suspended on a silicon frame (280 μm thickness, 9×9 mm^2) were fabricated by selective KOH etch of SiN_x-coated Si wafers. Thin photoresist films were spin-coated on membranes to achieve one or more target thickness and subsequently baked at 80°C for 2 min to remove the solvent.

The absorption coefficient was measured for nonchemically amplified metal-based photoresists synthesized at the Advanced Research Center for Nanolithography (ARCNL). Tin-oxo cages, with five different counterions, were functionalized as negative-tone photoresists for EUV, to achieve high absorbance and high etch resistance. The chemical equation of the basic building blocks was: $[(C_4H_9Sn)_{12}O_{14}(OH)_6]X_2$, and is schematically shown in Fig. 3. The tin cages were prepared as previously described in the literature.[26–28] The counterions X were tosylate $CH_3C_6H_4SO_3^-$ (Sn-S), hydroxide OH^- (Sn-OH), acetate CH_3COO^- (Sn-A), malonate $CH_2(COO)_2^{2-}$ (Sn-M), and trifluoroacetate CF_3COO^- (Sn-F). Sn-F contains fluorine, and it is therefore expected to have a slightly higher absorbance than the others. The patterning performance of these materials with EUV radiation has been recently studied and showed a good potential for high resolution and high sensitivity.[29] In addition, the chemical changes upon DUV exposure were studied for these materials and a chemical mechanism for the observed changes was proposed.[30]

A commercial zirconium oxocluster (ZrM1) was purchased from Sigma-Aldrich (CAS 189028-53-3) and used as it is, aside from the dilution, which was tuned to attain different thicknesses. A different zirconium oxocluster (ZrM2) and a hafnium methacrylate oxocluster (HfM) were prepared as described in previous works.[31,32] In this latter case, $Zr(O^iPr)_4$ and $Hf(OBu)_4$ were mixed with methacrylic acid in acetonitrile and kept at room temperature. The formed crystals were filtered off and washed with acetonitrile. Thermogravimetric analyses, nuclear magnetic resonance and infrared spectroscopy, and powder x-ray diffraction experiments, detailed elsewhere,[31,32] indicated that the compounds consisted of inorganic oxoclusters with four to six metallic atoms. Schematic structures of the ZrM2

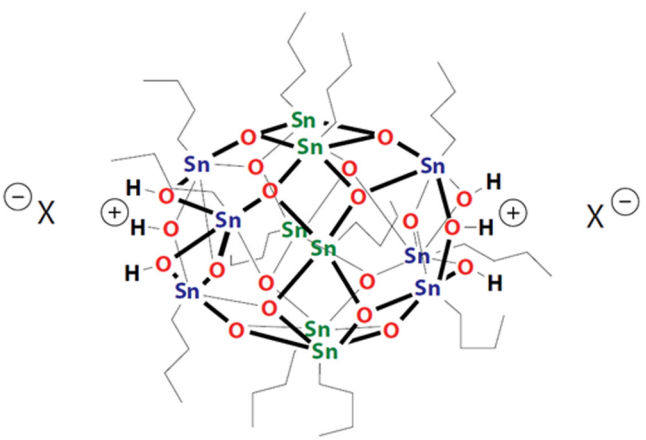

Fig. 3 Schematic of tin cages structures. The counterions are indicated by the X (see text for detailed description).

Downloaded From: https://www.spiedigitallibrary.org/journals/Journal-of-Micro/Nanolithography,-MEMS,-and-MOEMS on 08 May 2019
Terms of Use: https://www.spiedigitallibrary.org/terms-of-use

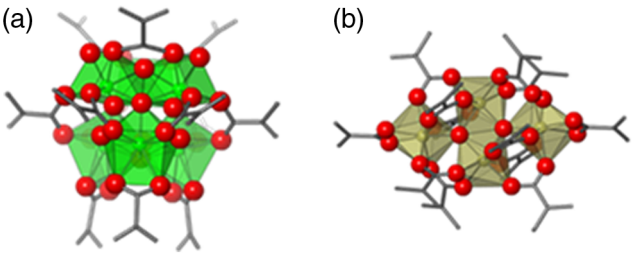

Fig. 4 Schematic of (a) Zr-based and (b) Hf-based oxoclusters structures. (a) Green or (b) brown polyhedra delimit the coordination geometry of Zr and Hf atoms, respectively. Red balls represent oxygen atoms and gray bars represent carbon–carbon bonds.

Table 1 Description of metal oxides photoresists: manufacturer, type, and metal.

Sample	Manufacturer	Type	Metal
Sn-M	ARCNL	Cage	Sn
Sn-A	ARCNL	Cage	Sn
Sn-F	ARCNL	Cage	Sn
Sn-S	ARCNL	Cage	Sn
Sn-OH	ARCNL	Cage	Sn
ZrM1	Sigma-Aldrich	Oxocluster	Zr
ZrM2	ARCNL	Oxocluster	Zr
HfM	ARCNL	Oxocluster	Hf

and HfM are shown in Fig. 4. For all the aforementioned metal-based materials, the theoretical absorption is determined by the elemental composition and from the estimation of the density of the spin-coated films based on the crystal structures and accounting for the packing ratio. The description of samples is provided in Table 1.

2.4 *Spectroscopic Ellipsometry*

The accurate measurement of the thickness of a photoresist coated on a suspended membrane is technically challenging, and it is the major source of uncertainty in the estimation of α. In general, the thickness at which a photoresist coats in a spinner depends on the substrate material, but it is typically predictable. In our specific case, spin coating on a membrane adds a significant uncertainty to the final thickness, which thus needs to be measured for each sample individually. Profilometry and atomic force microscopy cannot be used to measure the morphology on such thin membranes. For this reason, we relied on optical measurement by use of an M-2000 spectroscopic ellipsometer from J. A. Woollam, equipped with a 75 W Xe ARC light source. The spectral range was 250 to 1000 nm and the spot size was about 300 μm in diameter. Ellipsometric measurements were performed on 25 different spots on the sample, on a square area of 1×1 mm^2 with a step size of 0.2 mm. The ellipsometric data were modeled as two layers: for the SiN_X membrane using a SiN_X (Cody–Lorentz) model and for the resist layer using a Cauchy model. Because the optical constants of SiN_x and the resist layer were unknown, these were independently measured first. This was done by measuring angle scans of SiN_x on Si and the resist layer on Si. Initial material fits and optical constants of the SiN_x membrane were generated by angle scan on the Si frame surrounding the suspended membrane. For the resist layer, angle scans were preliminarily carried out to measure the optical constants by spin coating each photoresist on bulk Si wafers. Neither additional layers nor interfaces were needed to obtain a good fitting to the data. Furthermore, the same material was spin-coated and analyzed at several thickness ranges. This approach significantly reduces the uncertainty in the α, using a combination of optical inspection and spectroscopic ellipsometry to estimate d in the proximity of the exposed area.

2.5 *Estimation of Uncertainty*

The uncertainty in the measurement of α arises from three sources. The first source is the uncertainty in the measurement of the resist thickness (σ_d), due to the nonuniformity of the coating. The second is the uncertainty in the thickness of the SiN_x membrane, due to the variability in the deposition process, which affects the value of the reference photocurrent (σ_{I_0}). The third is the uncertainty in the measured photocurrent from the photodiode (σ_I). The standard deviation of α can be determined from the well-known equation for error propagation and replacing the due quantities

$$\sigma_\alpha = \sqrt{\left(\frac{\partial\alpha}{\partial d}\right)^2\sigma_d^2 + \left(\frac{\partial\alpha}{\partial I_0}\right)^2\sigma_{I_0}^2 + \left[\frac{\partial\alpha}{\partial I(t)}\right]^2\sigma_{I(t)}^2}$$
$$\cong \sqrt{\left(\frac{\partial\alpha}{\partial d}\right)^2\sigma_d^2 + \left(\frac{\partial\alpha}{\partial I_0}\right)^2\sigma_{I_0}^2} = \sqrt{\alpha^2\frac{\sigma_d^2}{d^2} + \frac{1}{d^2}\frac{\sigma_{I_0}^2}{I_0^2}}. \quad (3)$$

The approximation in Eq. (3) arises from the observation that fluctuations in measured photocurrent (σ_I) were negligible in comparison to all the other terms and, therefore, shall not be considered.

As mentioned above, samples for absorption measurement were prepared by spin coating each material to several target thicknesses. By doing so, we can verify whether the condition of homogeneous absorption is satisfied and Eq. (1) holds valid, provided that the logarithm of transmittance varies linearly with the film thickness. As a result, a linear fitting can be carried out to the measured log T_X data, the slope of which determines the absorption coefficient α. Each data point accounts for the standard deviation along both the abscissa and the ordinate that represent the uncertainty in transmittance T_X and thickness d, respectively. When more than one thickness is available, the standard deviation of α is estimated as the standard deviation of the slope of the least-squares linear fit to the data. This is calculated using the instrumental weighting on the uncertainties of both axes according to a numerical implementation of a method described elsewhere.[33] When a given sample is available at only one given thickness, the uncertainty of α is extracted from Eq. (3) instead.

Downloaded From: https://www.spiedigitallibrary.org/journals/Journal-of-Micro/Nanolithography,-MEMS,-and-MOEMS on 08 May 2019
Terms of Use: https://www.spiedigitallibrary.org/terms-of-use

3 Results and Discussion

Metal-containing photoresists offer several advantages for EUV lithography in comparison to conventional organic platforms. Primarily, these photoresists are negative tone and can be exploited as directly patternable hard masks owing to the high etching resistance. In hybrid oxide resists, the exposure mechanism probably proceeds by detachment (and outgassing) of the organic ligands, whereas the metal (core or hydroxide) condenses and grows into a pseudo-oxide network.[34]

For the absorption measurement, metal-based photoresists from ARCNL have been coated at thicknesses ranging from 11 to 76 nm. The transmittance, T_X, was measured and is plotted in Fig. 5 as a function of the measured thickness, d, of each individual coated membrane. Notably, it can be observed that all samples studied in this work exhibited a linear $\ln(T_X)$ versus d trend. It is thus appropriate to extract the α as the slope of the linear fit to the data, according to the methodology described in Sec. 2.5. The five variants of tin cage only differ in the type of counterion group. For the zirconium compounds, we compared the material synthesized at ARCNL with that from the manufacturer Sigma-Aldrich. Only one thickness was available for Hf-containing material, and its α was extracted from a single membrane thickness measurement.

The experimental α values for all the metal-containing resists are shown in Fig. 6. As a matter of comparison, the absorption coefficient of a typical organic CAR (4.8 μm^{-1})[22,35] is also shown (Fig. 6, gray bar). Depending on the counterion, α was 14.7 μm^{-1} (malonate), 14.2 μm^{-1} (acetate), 11.6 μm^{-1} (trifluoroacetate), 11.1 μm^{-1} (tosylate), and 10.9 μm^{-1} (hydroxide). In sum, the absorption coefficient of the tin cages compounds was found to be about two to three times higher than that of conventional CAR resists based on an organic backbone. This finding is ascribed to the large absorption cross section of tin at EUV and to the relatively large amount of this element in the compound. This finding is also consistent with and comparable to that reported previously on tin-based organo-oxo molecules, where α was measured between 15 and 19 μm^{-1}.[22] In these tin cage systems, absorption also shows some dependence on the counterion group. Contrary to expectations, higher absorption of the fluorine-containing Sn-F (trifluoroacetate counterions) compared to Sn-A (acetate counterions) was not observed experimentally. A reason could be a lower density of the coated Sn-F film compared to Sn-A due to, for instance, a small amount of solvent trapped in the film or different packing arrangement. Furthermore, the counterions constitute only a small fraction of the absorption considering the strongly absorbing Sn atoms. Further study is envisioned to clarify how the counterion structure affects the packing density of the material after spin coating and, therefore, its effect on optical absorption.

Compared to the tin-containing compounds, the enhancement in EUV absorption was not as significant in zirconium-containing ones, where the absorption was only slightly higher than in conventional CAR. This result is ascribed to the relatively small absorption cross section of Zr in comparison to oxygen and carbon, the main constituents of organic resists. There was not a sizeable difference, within experimental error, between the commercial compound (ZrM1) and the one prepared in house (ZrM2). As for the hafnium-based material HfM, it showed about 9.0 μm^{-1} absorption, which is due to the good absorptivity of the element than conventional organic resists. In the case of the HfM sample, only one thickness sample was available

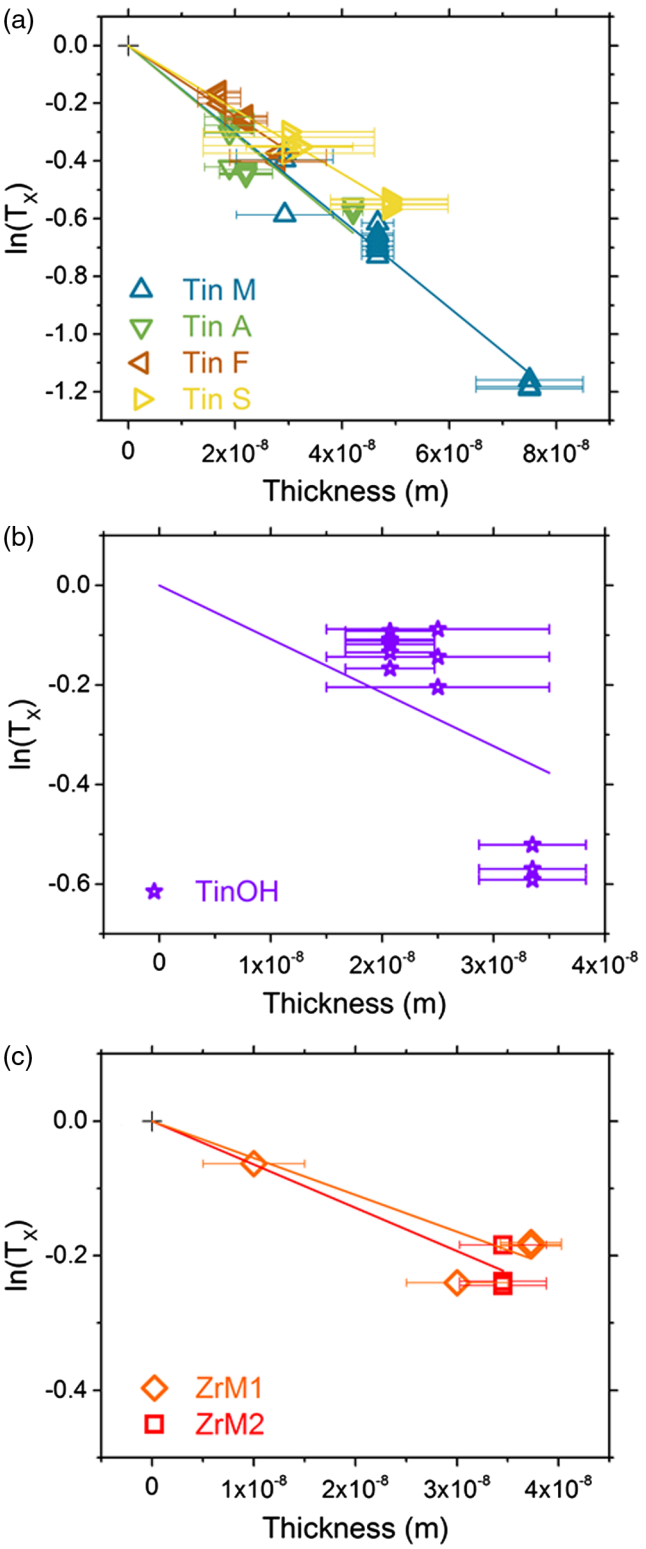

Fig. 5 Logarithm of transmittance as a function of resist film thickness for all the metal oxide photoresists synthesized at ARCNL and based on (a), (b) tin cages, and (c) zirconium oxoclusters. The solid lines are the least-squares linear fit to the data.

Downloaded From: https://www.spiedigitallibrary.org/journals/Journal-of-Micro/Nanolithography,-MEMS,-and-MOEMS on 08 May 2019
Terms of Use: https://www.spiedigitallibrary.org/terms-of-use

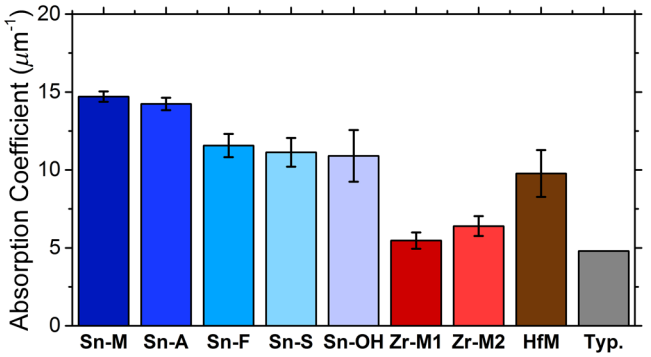

Fig. 6 Summary of measured linear absorption coefficient α of metal oxide photoresists at EUV: tin cages with different counterions (shades of blue), zirconium oxoclusters (shades of red), and hafnium oxocluster (brown). The uncertainty of α is shown as error bar. The absorption of a typical chemically amplified organic photoresist at EUV is also shown for comparison (gray).

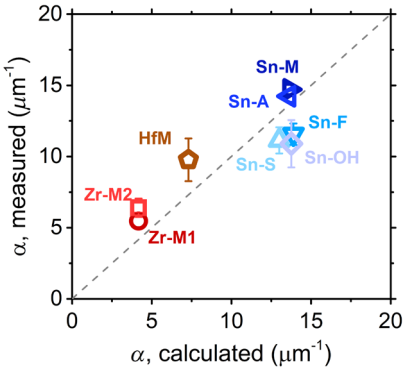

Fig. 7 Comparison of measured linear absorption coefficient α versus estimated α for metal-based photoresists synthesized at ARCNL.

for measurement: for this reason, no linear fit is shown in Fig. 5, and the associated error bar (Fig. 6) is significantly larger than that of the other samples.

The theoretical values of the absorption coefficient were estimated from elemental absorption cross sections at 92 eV,[16] weighted on the relative amount of each element and the density of the material according to the well-known equation

$$\alpha = \frac{N_A \sum_n x_n \sigma_{a_n}}{MW} \rho, \tag{4}$$

where N_A is Avogadro number, MW is the molecular weight of the compound, n is the number of elements in the compound, x_n is the relative amount of the n'th element, σ_{a_n} is the absorption cross section of the n'th element, and ρ is the density. The density plays a key role in the absorptivity, as Eq. (4) shows. ρ was estimated from the crystal structure of the material and taking into account the packing arrangement. Typically, organic photoresists have a density comparable to that of the polymer backbone: 1.14 g/cm^3 (polymethylmethacrylate) or 1.03 g/cm^3 (polystyrene).[36] The tin cages have been calculated to have a density of 1.93[26] or 1.84 g/cm^3.[37] The density of the zirconium oxocluster is 1.16 g/cm^3,[31] whereas 1.9 g/cm^3 for the hafnium oxocluster.[32]

The comparative plot in Fig. 7 shows a good agreement between the experiment and estimate. For the tin cages with trifluoroacetate, tosylate, and hydroxide, the measured absorptivity was slightly lower than the expected value. For instance, the estimated absorption of the Sn-F is 13.9 μm^{-1} compared to 13.6 μm^{-1} for Sn-A, whereas our experimental measurement showed an opposite trend (Sn-A more absorbing than Sn-F). For the Hf- and Zr-based materials, the experimental α was higher than the value expected from the elemental composition. The discrepancies are ascribed to differences in the actual density of the film after spin coating. In summary, the actual absorption can be different from the expected value, and this can affect the resulting lithographic sensitivity and performance of the photoresist.

4 Conclusions

The absorption coefficients at the EUV wavelength of 13.5 nm of hybrid metal oxo-compounds have been measured experimentally using a dedicated instrumentation setup and synchrotron light source. By preparing a series of thickness, the α was measured with unprecedented accuracy. It was found that tin cage resists have a very high absorptivity in the EUV, two to three times higher than that of conventional CARs based on organic polymers. The measured absorption of these tin cage materials is also comparable to that of other tin organo-oxo molecular resists. The measured absorption of zirconium oxocluster photoresist was comparable to that of organic photoresists, a finding that can be ascribed to the low contribution of Zr to the overall absorption cross section of the material, and to the similar density of these materials. The hafnium-containing oxoclusters showed a higher absorptivity than those based on zirconium, owing to the larger absorption cross section of Hf.

The estimated absorptivity was then calculated from the film density and the tabulated atomic cross sections. The experimental and the estimated α values were in fairly good agreement. The predictability of the linear absorptivity in molecular inorganic photoresists represents added value to this new type of materials. We ascribe the observed discrepancy of the absorption coefficients to the difference between the actual film density and the quoted values, which mostly assume a densely packed crystalline form of the material while the spin-coated materials are mostly not crystalline and can contain solvent or voids. The accurate measurement of the absorption of the EUV resists is of crucial importance for further development of EUV resists and for more accurate lithographic modeling. The developed method here can contribute to these by providing precise values of absorption constant of EUV materials.

Acknowledgments

We kindly acknowledge the technical support of Michaela Vockenhuber and Markus Kropf (PSI). Part of this work has been carried out at the Advanced Research Center for Nanolithography (ARCNL), a public–private partnership of the University of Amsterdam (UvA), the VU University Amsterdam (VU), the Netherlands Organization for Scientific Research (NWO), and the semiconductor equipment manufacturer ASML. Spectroscopic ellipsometry has been carried out with the technical support of Goran

Downloaded From: https://www.spiedigitallibrary.org/journals/Journal-of-Micro/Nanolithography,-MEMS,-and-MOEMS on 08 May 2019
Terms of Use: https://www.spiedigitallibrary.org/terms-of-use

Milinkovic and Pieter-Jan van Zwol (ASML). Part of this work was performed at Swiss Light Source. Parts of this work have been published as an SPIE Proceeding paper [R. Fallica, J. Haitjema, L. Wu, S. Castellanos, F. Brouwer, Y. Ekinci, Extreme Ultraviolet (EUV) Lithography VIII, edited by Eric M. Panning, Kenneth A. Goldberg, Vol. 10143, 101430A © 2017 SPIE].

References

1. E. Buitrago et al., "Chapter 4: EUV lithography process challenges," in *Frontiers of Nanoscience*, A. Robinson and R. Lawson, Eds., Vol. 11, pp. 135–176, Elsevier, Amsterdam, Netherlands (2016).
2. J. W. Thackeray et al., "Deep UV ANR photoresists for 248 nm excimer laser photolithography," *Proc. SPIE* **1086**, 34–46 (1989).
3. A. Sekiguchi et al., "Measurement of parameters for simulation of deep-UV lithography using an FT-IR baking system," *Proc. SPIE* **3678**, 985–1000 (1999).
4. A. C. Cefalas et al., "Absorbance and outgasing of photoresist polymeric materials for UV lithography below 193 nm including 157 nm lithography," *Microelectron. Eng.* **53**, 123–126 (2000).
5. J. F. Cameron et al., "Comparison of acid-generating efficiencies in 248 and 193-nm photoresists," *Proc. SPIE* **4345**, 106–118 (2001).
6. L. Li et al., "Extreme ultraviolet resist materials for sub-7 nm patterning," *Chem. Soc. Rev.* **46**, 4855–4866 (2017).
7. T. Kozawa and S. Tagawa, "Radiation chemistry in chemically amplified resists," *Jpn. J. Appl. Phys.* **49**, 030001 (2010).
8. A. Pirati et al., "EUV lithography performance for manufacturing: status and outlook," *Proc. SPIE* **9776**, 97760A (2016).
9. C. D. Higgins et al., "Resolution, line-edge roughness, sensitivity trade-off, and quantum yield of high photo acid generator resists for extreme ultraviolet lithography," *Jpn. J. Appl. Phys.* **50**, 036504 (2011).
10. E. Zanchetta et al., "Novel hybrid organic-inorganic spin-on resist for electron- or photon-based nanolithography with outstanding resistance to dry etching," *Adv. Mater.* **25**, 6261–6265 (2013).
11. S. Chakrabarty et al., "Oxide nanoparticle EUV resists: toward understanding the mechanism of positive and negative tone patterning," *Proc. SPIE* **8679**, 867906 (2013).
12. D. De Simone et al., "Novel metal containing resists for EUV lithography extendibility," *Proc. SPIE* **9776**, 977606 (2016).
13. J. Stowers et al., "Metal oxide EUV photoresist performance for N7 relevant patterns and processes," *Proc. SPIE* **9779**, 977904 (2016).
14. J. K. Stowers et al., "Directly patterned inorganic hardmask for EUV lithography," *Proc. SPIE* **7969**, 796915 (2011).
15. M. van de Kerkhof et al., "Enabling sub-10 nm node lithography: presenting the NXE:3400B EUV scanner," *Proc. SPIE* **10143**, 101430D (2017).
16. B. L. Henke, E. M. Gullikson, and J. C. Davis, "X-ray interactions: photoabsorption, scattering, transmission, and reflection at E = 50–30000 eV, Z=1–92," *At. Data Nucl. Data* **54**(2), 181–342 (1993).
17. C. Popescu et al., "Sensitivity enhancement of the high-resolution xMT multi-trigger resist for EUV lithography," *Proc. SPIE* **10143**, 101430V (2017).
18. A. Sekiguchi et al., "Study of Dill's B parameter measurement of EUV resist," *Proc. SPIE* **9422**, 94222L (2015).
19. S. Grzeskowiak et al., "Analytical techniques for mechanistic characterization of EUV photoresists," *Proc. SPIE* **10146**, 101462C (2017).
20. Y.-J. Kwark et al., "Absorbance measurement of polymers at extreme ultraviolet wavelength: correlation between experimental and theoretical calculations," *J. Vac. Sci. Technol. B* **24**, 1822 (2006).
21. S. Irie et al., "Study of transmittance of polymers and influence of photoacid generator on resist transmittance at extreme ultraviolet wavelength," *Jpn. J. Appl. Phys. Pt. 1* **41**(9), 5864–5867 (2002).
22. R. Fallica et al., "Dynamic absorption coefficients of chemically amplified resists and nonchemically amplified resists at extreme ultraviolet," *J. Micro/Nanolithogr. MEMS MOEMS* **15**(3), 033506 (2016).
23. J. Haitjema et al., "Photoreactions of Tin oxo cages, model EUV photoresists," *J. Photopolym. Sci. Technol.* **30**, 99–102 (2017).
24. N. Mojarad et al., "Single-digit-resolution nanopatterning with extreme ultraviolet light for the 2.5 nm technology node and beyond," *Nanoscale* **7**, 4031–4037 (2015).
25. P. Helfenstein et al., "Scanning coherent diffractive imaging methods for actinic extreme ultraviolet mask metrology," *J. Micro/Nanolithogr. MEMS MOEMS* **15**(3), 034006 (2016).
26. C. Eychenne-Baron, F. Ribot, and C. Sanchez, "New synthesis of the nanobuilding block $\{(BuSn)_{12}O_{14}(OH)_6\}^{2+}$ and exchange properties of $\{(BuSn)_{12}O_{14}(OH)_6\}(O_3SC_6H_4CH_3)_2$," *J. Organomet. Chem.* **567**(1–2), 137–142 (1998).
27. L. van Lokeren et al., "Probing the anions mediated associative behavior of tin-12 oxo-macrocations by pulsed field gradient NMR spectroscopy," *J. Phys. Chem.* **114**, 16087–16098 (2010).
28. B. Cardineau et al., "Photolithographic properties of tin-oxo clusters using extreme ultraviolet light (13.5 nm)," *Microelectron. Eng.* **127**, 44–50 (2014).
29. J. Haitjema et al., "Tin-oxo cages for use as photoresists in EUV lithography," *J. Micro/Nanolithogr. MEMS MOEMS* **16**, 033510 (2017).
30. Y. Zhang et al., "Photochemical conversion of a tin-oxo cage compound studied using hard x-ray photoelectron spectroscopy," *J. Micro/Nanolithogr. MEMS MOEMS* **16**, 023510 (2017).
31. G. Kickelbick and U. Schubert, "Oxozirconium methacrylate clusters: $Zr_6(OH)_4O_4(OMc)_{12}$ and $Zr_4O_2(OMc)_{12}$ (OMc = Methacrylate)," *Chem. Ber.* **130**, 473–478 (1997)
32. S. Gross et al., "Mono-, di-, and trimetallic methacrylate-substituted metal oxide clusters derived from hafnium butoxide," *Monatshef. Chem.* **134**, 1053–1063 (2003).
33. D. York et al., "Unified equations for the slope, intercept, and standard errors of the best straight line," *Am. J. Phys.* **72**(3), 367–375 (2004).
34. W. D. Hinsberg and S. Meyers, "A numeric model for the imaging mechanism of metal oxide resists," *Proc. SPIE* **10146**, 1014604 (2017).
35. N. N. Matsuzawa et al., "Theoretical estimation of absorption coefficients of various polymers at 13 nm," *Microelectron. Eng.* **53**, 671–674 (2000).
36. B. Watts et al., "Nanoscale measurement of the absolute mass density of polymers," *Phys. Status Solidi A* **212**, 518–522 (2015).
37. C. Eychenne-Baron et al., "Reaction of butyltin hydroxide oxide with p-toluenesulfonic acid: synthesis, x-ray crystal analysis, and multinuclear NMR characterization of $\{(BuSn)_{12}O_{14}(OH)_6\}(4\text{-}CH_3C_6H_4SO_3)_2$," *Organometallics* **19**, 1940–1949 (2000).

Biographies for the authors are not available.

Downloaded From: https://www.spiedigitallibrary.org/journals/Journal-of-Micro/Nanolithography,-MEMS,-and-MOEMS on 08 May 2019
Terms of Use: https://www.spiedigitallibrary.org/terms-of-use